ORIGINAL PAPER

A novel two-layer winding topology for sub-harmonic synchronous machines

S. M. Sajjad Hossain Rafin[1,2] · **Qasim Ali[3]** · **Sajid Khan[4]** · **Thomas A. Lipo[5]**

Abstract

With optimized design and modern brushless operation, wound rotor synchronous machines are resurrecting as a strong contender in many applications presently dominated by permanent magnet machines. Considering the notion, this paper introduces a novel brushless synchronous machine topology that utilizes sub-harmonic magnetomotive force (MMF) of its stator winding for desirable brushless operation. It is significant to state that the sub-harmonic MMF component that is used in this novel topology is one-fourth of the fundamental MMF component, whereas, in previous practices, it was half. Moreover, the stator of the machine uses a new winding arrangement of two sets of balanced three-phase windings wound in two layers to produce the fundamental and the sub-harmonic MMF. To achieve the brushless excitation, the rotor utilizes an additional winding that is used to induce the electromotive force (EMF) by the sub-harmonic MMF component of the stator. This novel two-layer stator winding topology permits the utilization of maximum allowable space in the stator to house conductors in all of its 48 slots, which was not the case in previous papers. To validate the performance, and feasibility, an 8-pole 48-slot brushless wound rotor synchronous motor is designed, and a 2-D finite element analysis simulation is conducted, where the topology shows immense potential in terms of better torque performance.

Keyword Brushless excitation systems · Sub-harmonic excitation · Synchronous machines · Two-layer winding · Sub-harmonic synchronous machines

Abbreviations

MMF	Magnetomotive force
EMF	Electromotive force
EV	Electric vehicle
HEV	Hybrid electric vehicle
PMSM	Permanent magnet synchronous machines
IM	Induction motors
SRM	Switched reluctance motor
PM	Permanent magnet
WRSM	Wound rotor synchronous machines
SH	Sub-harmonic
SH-MMF	Sub-harmonic magnetomotive force
BL-WRSM	Brushless wound rotor synchronous machine
SHSM	Sub-harmonic synchronous machine
2-D FEA	2 Dimensional finite element analysis
LSHSM-01	Lipo sub-harmonic synchronous machine-01

✉ S. M. Sajjad Hossain Rafin
sajjad.rafin@griffithuni.edu.au, rafin.sajjad@gmail.com

1 School of Engineering and Built Environment, Griffith University, Gold Coast, QLD, Australia

2 Department of Electrical and Electronic Engineering, Northern University Bangladesh, Dhaka, Bangladesh

3 Department of Electrical Engineering, Sukkur IBA University, Sukkur, Pakistan

4 Center of Excellence for Robotics, Artificial Intelligence and Blockchain, Sukkur IBA University, Sukkur, Pakistan

5 Department of Electrical and Computer Engineering, University of Wisconsin Madison, Madison, WI, USA

1 Introduction

Electric machines, one of the core components of the electrified transportation system, and its technologies have been broadly researched particularly in machine topologies, characteristics, control strategies, and performance evaluations [1–5]. Although induction machines have been in the electrified transportation market for a long time, permanent magnet synchronous machines (PMSMs) have taken their

place because of higher torque density and efficiency [1, 3]. Despite the advantages, the high cost of rare earth magnets and the fixed flux nature make them an unattractive choice. To find alternatives, extensive research and development works are going on regarding synchronous machines that have reduced or absent permanent magnets [6, 7]. Evidently, the PM-assisted or the PM-less switched reluctance motors possess traits of induction motors and PMSMs in terms of robustness, efficiency, and power density [8].

To seek additional alternatives to PMSMs, brushless wound rotor synchronous machines (BL-WRSM), both PM-less and PM-assisted, are becoming popular among researchers for their controllability and simple excitation system [7]. Apart from brushless exciters and rotating transformers, three advanced brushless field excitation methods were developed in recent times: harmonic, inductive, and capacitive power transfer [7]. To discover the feasibility of sub-harmonic and higher-order harmonic MMF for the brushless operation of the wound rotor synchronous machines (WRSMs), a handful of investigations are done [8–12]. However, the higher-order harmonics generated from 3-phase stator MMF were used in a WRSM encounters additional harmonic losses [8].

Realizing the sub-harmonic MMF method, a dual inverter BL-WRSM topology was presented in [9] where both inverters provide two sets of currents to the stator winding in order to generate fundamental and sub-harmonic rotating magnetic field. On the rotor side, two separate winding is used, i.e., field winding and excitation winding, and among them, the excitation winding induces the sub-harmonic MMF (SH-MMF) component. The induced voltage is then rectified and feed to the field winding for the brushless operation to be completed. In order to improve torque density and starting ability, a PM-assisted BL-WRSM was introduced in [10].

Utilizing the SH-MMF component to achieve the brushless operation, another approach is introduced in [11] by using a novel stator winding arrangement, where one inverter is used instead of two for supplying the input current. Furthermore, this one inverter BL-WRSM's field and excitation windings use 8 and 4 poles arrangement respectively as opposed to 4 and 2 used in [9, 10]. Later in [12], an optimized rotor design was presented, where the performance of the machine was enhanced in terms of output power quality, reduced torque ripple, and higher average torque production. Although the machine performance was improved to some extent, the machines in [11, 12] are underutilized in terms of the slot space because of the stator winding arrangement. Moreover, in [13] a new sub-harmonic synchronous machine is proposed, where in the stator a novel three-layer winding was introduced. Out of the three windings, two layers are used for fundamental MMF production, and the third layer is utilized for sub-harmonic MMF production that is ultimately used for brushless operation of the synchronous machine.

With this objective in mind, this paper introduces a novel BL-WRSM having a unique two-layer stator winding arrangement that provides better performance than that of the BL-WRSMs presented in [11, 12] having the exact size, volume, and machine rating. The following sections of the paper will cover the structure, machine configuration, and working principle of the novel BL-WRSM. Along with these, a 2-D finite element analysis (2-D FEA) has been performed to test the validity of the machine. For proper identification, we, the

Fig. 1 Proposed brushless wound rotor synchronous machine topology
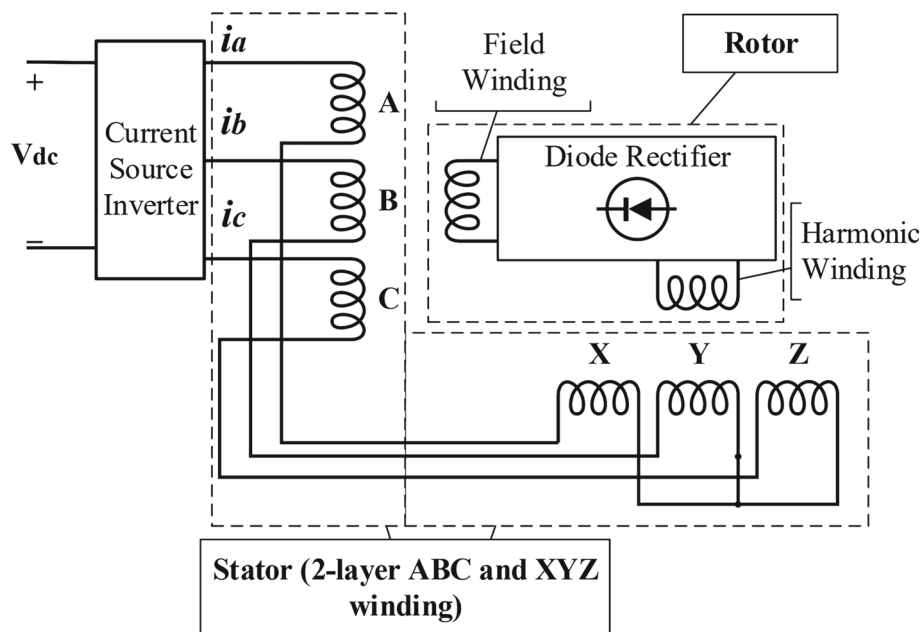
Fig. 2 Proposed LSHSM-01 layout and stator-rotor winding configuration
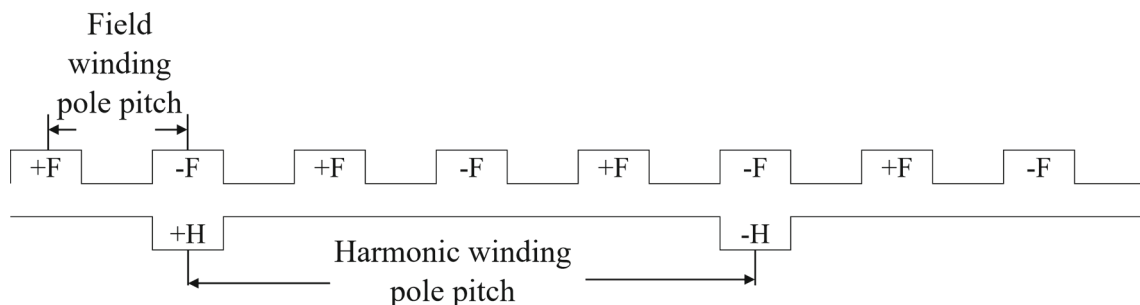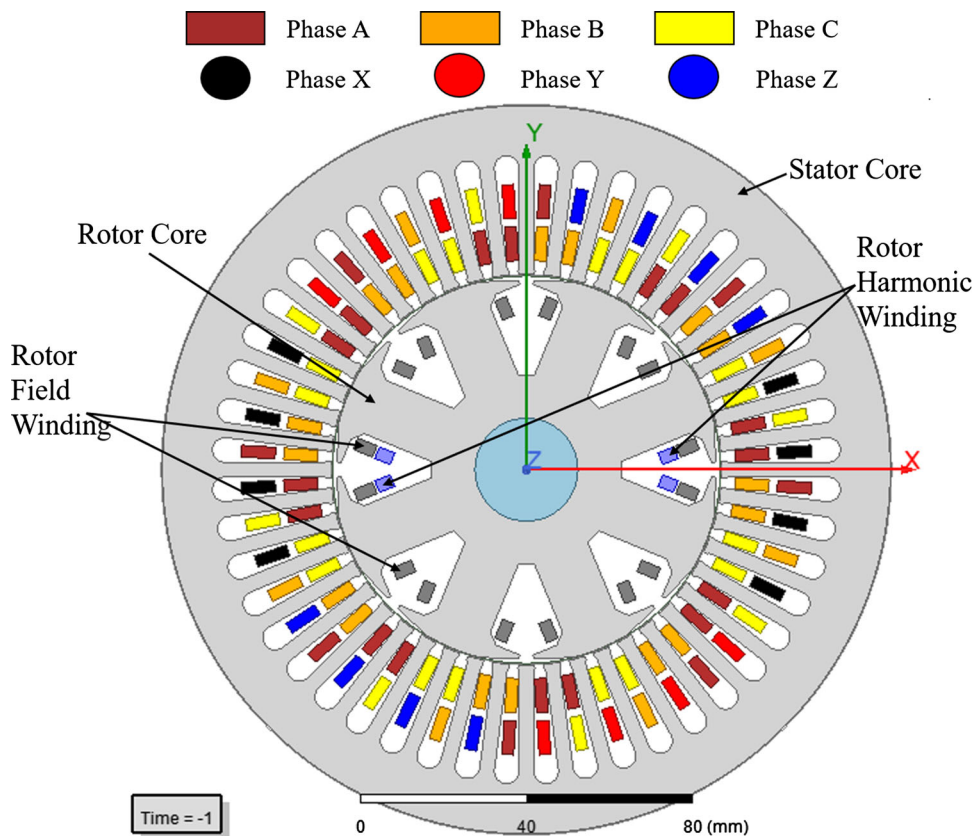
Fig. 3 Pole pitches of the 8-pole field and 2-pole harmonic windings of the rotor

author would like to name the machine: Lipo Sub-Harmonic Synchronous Machine 01 (LSHSM-01).

2 Proposed brushless topology and principle of operation

2.1 Proposed topology

The topology of the proposed LSHSM-01 is illustrated in Fig. 1, and it can be seen that the stator winding is driven by a single current source inverter. Moreover, the stator winding has a novel 2-layer distributed winding arrangement.

This two-layer winding is essentially two sets of series-connected 3-phase windings: ABC and XYZ. Furthermore, Fig. 2 depicts the machine layout with stator-rotor windings, and it is illustrated that the bottom layer of the stator slots is comprised of only ABC winding while the top layer consists of both ABC and XYZ winding, where the XYZ winding has alternative placement. Notably, winding ABC generates an 8-pole MMF, and winding XYZ produces a 2-pole MMF.

From Fig. 2 it can be seen that the rotor of the LSHSM-01 is also comprised of two windings: field winding and harmonic winding. Similar to the ABC winding, the field winding is wound in an 8-pole manner but a concentrated arrangement. The harmonic winding is a 2-pole concentrated winding that is employed for inducing the sub-harmonic
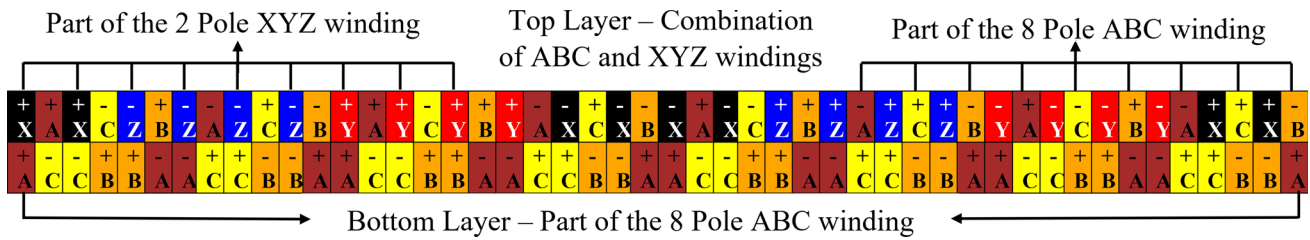
Fig. 4 Proposed 2-layer ABC and XYZ winding configuration over 360 mechanical degrees
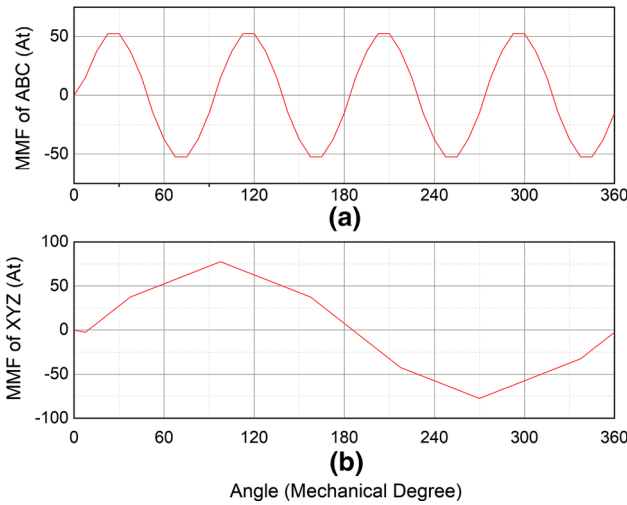

Fig. 5 **a** Fundamental component of the stator MMF and **b** Subharmonic component of the stator MMF

Table 1 Design parameters of the proposed LSHSM-01

Parameter	Unit	Value
Rated power	W	1281
Operating speed	rpm	900
Stator outer diameter	mm	177
Stator inner diameter	mm	95
Air-gap length	mm	0.5
Shaft diameter	mm	25
Stack length	mm	80
Number of poles of stator ABC winding	–	8
Number of poles of stator XYZ winding	–	2
Number of poles of rotor harmonic winding	–	2
Number of poles of rotor field winding	–	8
Number of stator slots	–	48
Conductors per stator slot in ABC winding	–	20 or 40
Conductors per stator slot in XYZ winding	–	20 or 00
Conductors per stator slot of harmonic winding	–	50
Conductors per stator slot of field winding	–	24

MMF generated by the 2-pole XYZ winding. To portray the structure of the rotor windings, Fig. 3 depicts the pole pitches of the field winding and the harmonic winding. Furthermore, a diode rectifier circuit is mounted on the periphery of the rotor as a bridge between the two rotor windings.

2.2 Principle of operation

As previously discussed, a balanced 3-phase current is supplied to the stator windings from a single current source inverter, and as the stator windings are series-connected, both ABC and XYZ windings receive an equal amount of currents from the inverter. The three-phase balanced current supplied by the inverter circuit is as follows,

$$
\begin{aligned}
i_a &= I \sin \omega_e t \\
i_b &= I \sin\left(\omega_e - \frac{2\pi}{3}\right) \\
i_c &= I \sin\left(\omega_e + \frac{2\pi}{3}\right)
\end{aligned}
\tag{1}
$$

where $i_a, i_b,$ and i_c are the three-phase supply currents, I is the peak supply current, ω_e is the electrical angular frequency, and t is the time.

Although the inverter supplies an equal amount of current to the stator windings, ABC and XYZ windings generate different MMF components because of their different pole numbers. Since the ABC winding is wound in an 8-pole manner, the winding generates the fundamental MMF component that is used for torque generation purposes. On the other hand, the XYZ winding generates its own MMF, but it is of a 2-pole configuration. Moreover, it can be observed that the 2-pole MMF component has quarter the frequency as that of the 8-pole MMF component; thus, the 2-pole component is termed as a sub-harmonic component, and this sub-harmonic MMF component is used for brushless field excitation. It is important to realize that the ABC and XYZ windings generate two distinct rotating magnetic fields that they rotate at a different speed than each other. Furthermore, Eqs. (2) and (3) can be utilized to compute the rotational speed of
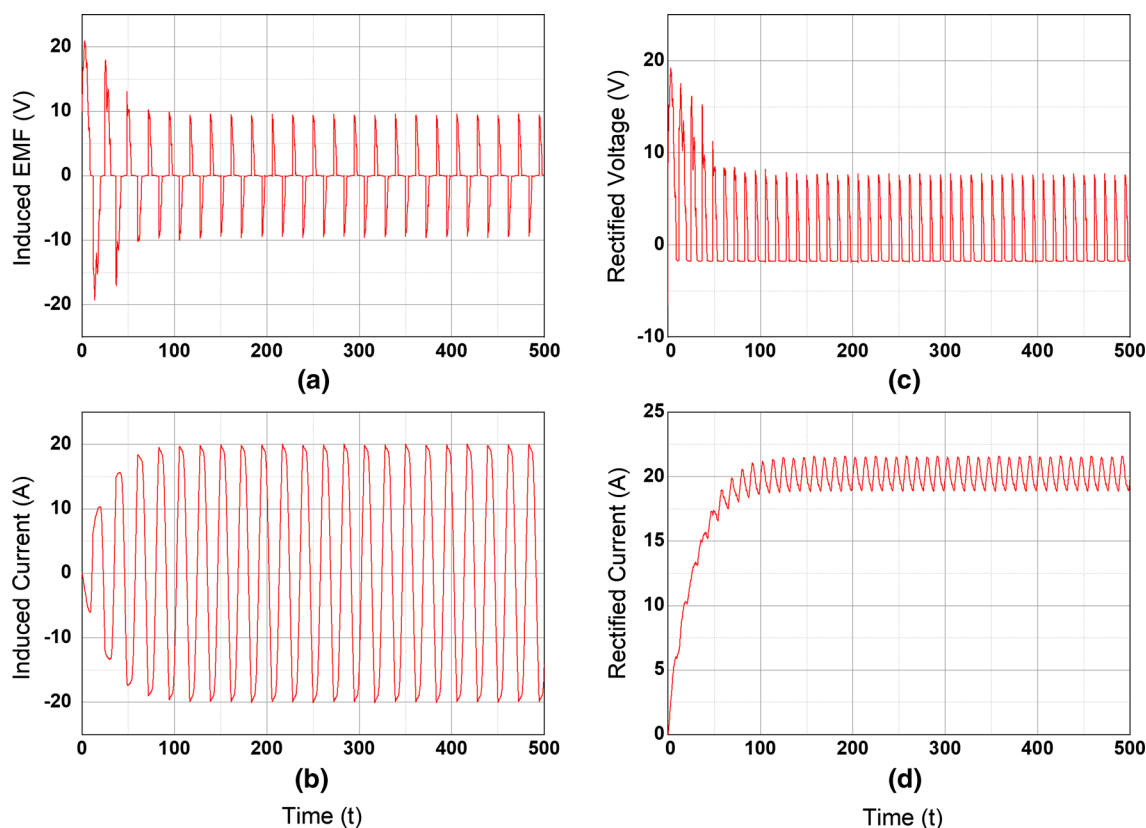
Fig. 6 Flux density plot through the stator, air-gap, and rotor
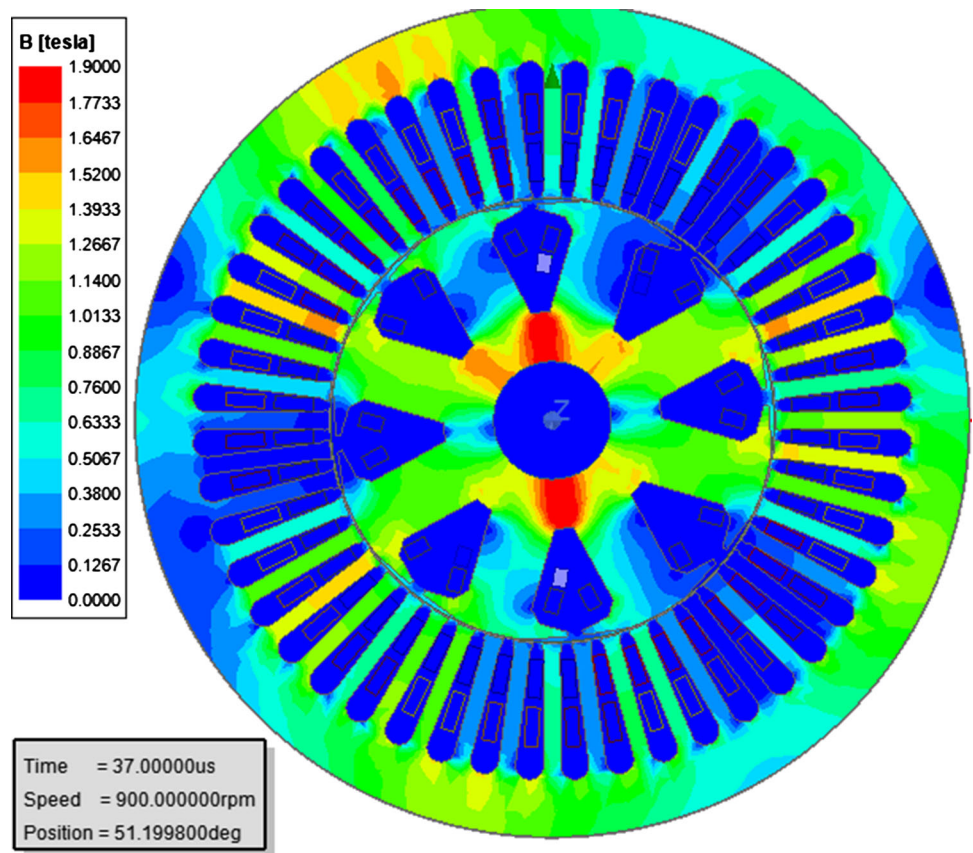
Fig. 7 Flux line distribution plot through the stator, air-gap, and rotor
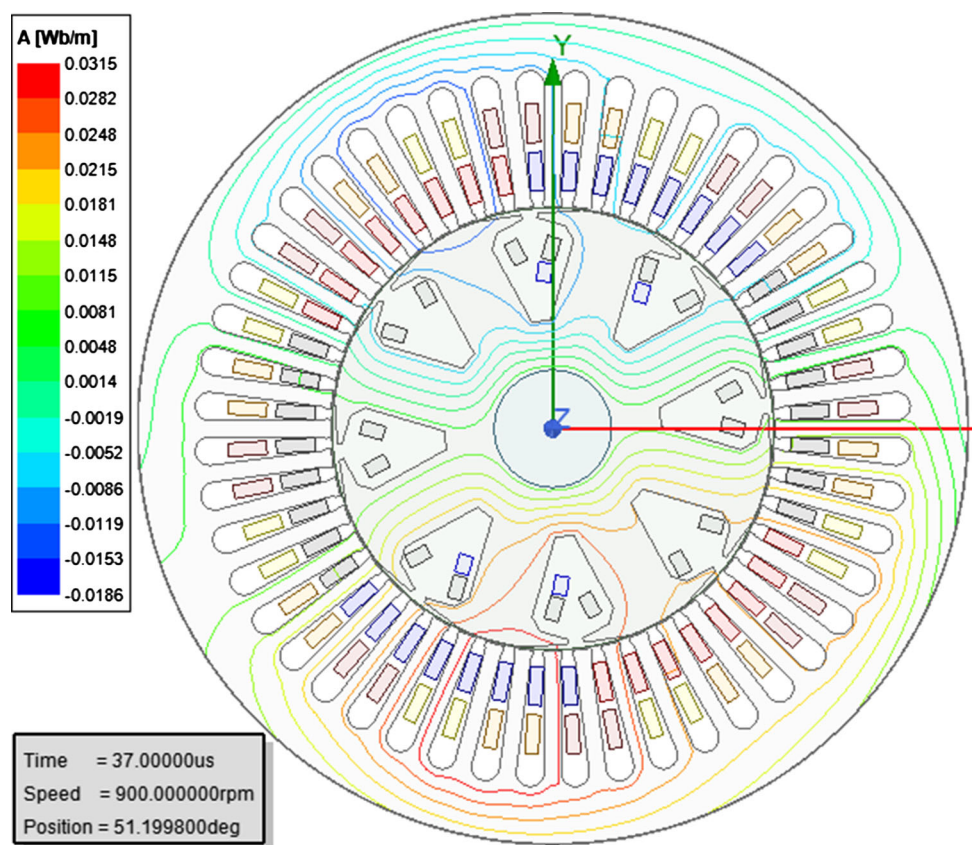
Fig. 8 **a** Induced voltage in the rotor harmonic winding, **b** current in the rotor harmonic winding, **c** rectified voltage in the rotor field winding, and **d** rectified current in the rotor field winding

the fundamental and harmonic components. They are as follows,

$$n_s = \frac{120 f}{p} \quad (2)$$

$$\eta_s(h) = \frac{n_s}{h} = \frac{120 f}{hp} \quad (3)$$

where n_s is the rotating speed of the fundamental component, f is the frequency of the supply current, p is the number of poles of the machine, $n_s(h)$ is the rotating speed of the harmonic component, and h is the harmonic number, which is 1/4 for the proposed case.

For an 8-pole machine, considering 60 Hz as the supply frequency, the fundamental MMF component rotates at 900 rpm that can be calculated using Eq. (2). Correspondingly, using Eq. (3), considering the value of h is 0.25, the rotating speed of the harmonic component is 3600 rpm. That authenticates the previously mentioned notion of having two different rotating speeds of the fundamental and harmonic component. To achieve the brushless operation, the harmonic winding of the rotor of the LSHSM-01 gets induced by the rotating SH-MMF generated by the stator XYZ winding. Subsequently, the induced EMF is rectified to DC voltage

by the means of a diode rectifier that ultimately feeds the 8-pole rotor field winding. With the DC excitation, the field winding creates a constant magnetic field that eventually is synchronized with the fundamental rotating magnetic field that is created by the ABC winding.

3 Design and analysis of the proposed machine

To validate the proposed LSHSM-01, an 8-pole, 48-slot, 3-phase machine is designed having a novel 2-layer distributed stator winding. Figure 4 illustrates the stator winding structure, which shows the 8-pole ABC and 2-pole XYZ windings that are placed throughout the 360° of the stator periphery. Each slot has two layers, and the ABC winding is wound in a unique two-layer manner where the bottom layer of the 48 slots are filled solely with the ABC winding; however, the top layer is wound in an alternative pattern, where 24 slots are wound with the ABC winding and the rest 24 slots are with the XYZ winding. More elaborately, for the top layer arrangement, if the 1st position of the top layer is wound with one of the ABC windings, the 2nd position is going to be wound with one of the XYZ windings. For example, it can

be seen from Fig. 4 that the very first position of the top layer is wound with "X+" conductors, the 2nd position is wound with "A+", the 3rd position is wound with "X+", the 4th position is with "C−", the 5th position is with "Z−", and so on in an alternating fashion throughout the 360° periphery.

Therefore, it can be stated that the ABC winding is wound in a semi two-layer manner, and the XYZ winding is wound in a semi single-layer manner. Eventually, the ABC and XYZ windings combinedly make a unique two-layer series-connected winding. If this exclusive two-layer winding is to be compared to the sub-harmonically excited two-layer winding presented in [9–12], it can be observed that the proposed 2-layer winding arrangement utilizes the optimal slot-space in 48 slots of the machine.

However, in [11, 12] the ABC and XYZ windings are housed separately in two equally divided slot-spaces in the stator, and winding ABC has doubled the number of turns than XYZ. Since the slots house different numbers of conductors in the different portions of the stator periphery, it causes a heating-imbalance throughout. In [9], the machine encounters a similar heating imbalance, for that reason, the author suggested supplying the high and low current alternatively by the two inverters at fixed intervals. Although the method may reduce the imbalance, it may impose newer complexity in the machine drive and control.

Provided that the proposed topology utilizes the maximum number of conductors per slot in the stator winding, and the slots may have either of the two combinations—winding ABC has 20 when it shares with XYZ which has also, or winding ABC has all 40 when it does not share slot XYZ. Thus, each slot will have 40 turns in either combination as opposed to the machines in [11, 12], wherein some portion of the slots the turn number is 40 and, in some slots, it is 20. Importantly, the 40 turns in each stator slot results in an equal amount of current circulation, which in return makes the LSHSM-01 generate greater torque without having the issue of heating imbalance as compared to [9–12].

Table 1 summarizes the design parameters of the LSHSM-01, where the rated power of the machine is 1281 W with a constant speed of 900 rpm. For this design, the MMF distribution of the ABC and XYZ windings are illustrated in Fig. 5a, b respectively, where the supply current peak amplitude of the phase A and X is 6.4 A, and at that instance, the supply current value of B, C, Y, and Z phases are 3.2 A. To elaborate, the mechanical frequency of the 8-pole ABC and 2-pole XYZ windings are ωm, and $(\omega m)/4$ respectively.

3.1 4. 2-D finite element analysis

The proposed machine, LSHSM-01, has been extensively investigated to observe the performance and feasibility by using 2-D FEA. Data from Table 1 are taken as the simulation parameters, and a single inverter is used to supply a
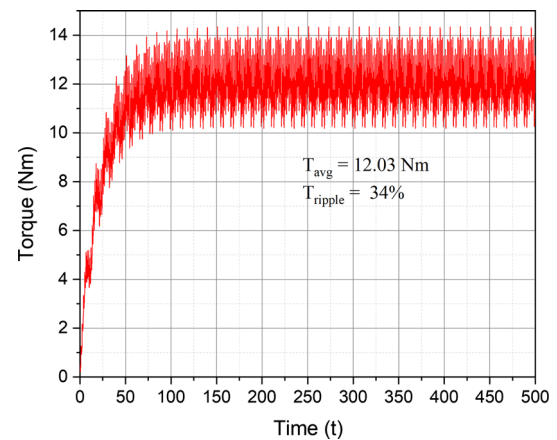

Fig. 9 Torque generation of the proposed LSHSM-01

balanced 3-phase sinusoidal current with a peak current of 6.4 A at a 60 Hz frequency. Figures 6 and 7 illustrate flux density and flux line distribution through the stator, air-gap, and rotor respectively. As mentioned earlier, the slots are filled evenly with the same number of conductors, as a result, the flux density and flux lines are also consistently distributed throughout the stator–airgap–rotor frame unlike in the case of BL-WRSM in [11, 12]. It is also important to point out that the proposed machine works equal and below the flux density level of 1.9 T continuously.

Furthermore, the induced EMF and the current in the rotor harmonic winding by the stator MMF from the XYZ winding are shown in Fig. 8a, b, and the values are 4.75 V and 14.78 A respectively. These alternating values are then rectified by a rectifier to supply the rotor field winding, and the average rectified voltage and current values are 0.63 V and 20.18 A respectively, which are shown in Fig. 8c, d. From these, it is apparent that the LSHSM-01 works on the principle of sub-harmonically excited brushless operation. Nevertheless, the performance of the LSHSM-01 could be further investigated in terms of its torque generation, and the average value is 12.03 Nm with a torque ripple of 34%, which is depicted in Fig. 9.

Further investigation is conducted to examine the effectiveness of the LSHSM-01 where the performance of the proposed machine is compared with the conventional WRSM used in [11] and the single inverter BL-WRSM in [12]. The summary of the evaluation is listed in Table 2, and it is important to state that all design parameters are kept the same to [12] which includes outer diameter, inner diameter, air-gap length, stack length, the current density in the stator, and rotor winding to name a few. Although three machines are supplied with the same RMS current of 4.5 A, the rotor field current of the LSHSM-01 (20.18 A) is found remarkably higher than the BL-WRSM (9.8 A) of [12]. The reasons for this higher current are the unique 2-layer stator winding

Table 2 Performance comparison between the conventional WRSM [11], BL-WRSM [12], and the proposed LSHSM-01

Indicator	Unit	WRSM [11]	BL-WRSM [12]	Novel LSHSM-01
Stator current	A_{rms}	4.50	4.50	4.50
Field current	A_{avg}	9.50	9.80	20.18
Harmonic current	A_{rms}	0	5.10	14.78
Terminal voltage	V_{rms}	68.10	72.03	91.75
Average torque	N m	7.30	7.83	12.03
Torque ripple	%	16.67	18.00	34
Stator winding copper loss	W	68.04	85.03	113
Field winding copper loss	W	51.60	57.62	97.73
Harmonic winding copper loss	W	0	7.80	8.3
Core loss	W	36.19	43.05	43.05
Efficiency	%	81.53	79.22	81.10

arrangement, the 2-pole sub-harmonic winding, and optimally utilized winding slot-space. As a result, the average torque of the LSHSM-01 is recorded 12.03 N m that is around 65% more than that of the machine in [12] having the same physical volume and design parameters. Although the torque is enhanced, torque ripple on the other hand is recorded as 34%, and this issue may be covered in future research with an optimized design. Moreover, calculating all the losses of these three machines, the efficiency of the novel machine is approximately 81%, which is exact compared to the conventional brushed WRSM of [11], but better than that of the similar sub-harmonic synchronous machine presented in [12] having efficiency of approximately 79%. Even though the efficiency is greater than the machine of [12], it can further be improved with optimized structural design and proper wire sizing selection.

4 Conclusion

The focal point of this paper is to develop a brushless wound rotor synchronous machine and study the performance and feasibility. For that, the proposed LSHSM-01 has substantiated with the 2-D FEA. Although operation wise it resembles the BL-WRSMs, performance-wise it surpasses in many crucial aspects demonstrating some certain advantages over the newly developed BL-WRSMs in [9–12]. Hence, the LSHSM-01 could be an alternative solution considering all the attractive features provided, and they are listed as follows:

1. Single inverter brushless operation.
2. Optimal utilization of the maximum slot space.
3. No unbalanced current circulation in the stator.
4. No need for imposing an unbalanced cooling system.
5. Greater torque generation.

With all these advantages, it can certainly be a competitive alternative not only to the BL-WRSMs but also with the state-of-the-art PMSMs particularly utilized in traction applications. It is equally important that the LSHSM-01 could potentially improve its performance by reducing the torque ripple through optimized design. In the power electronic drive and control section, scopes are there for improvement by utilizing the three-transistor voltage source inverter topology presented in [14] and employing various pulsed width modulation (PWM) techniques analyzed in [15]. Not to mention that these topics may be considered as future research concerns.

References

1. Pellegrino G, Vagati A, Boazzo B, Guglielmi P (2012) Comparison of induction and PM synchronous motor drives for EV application including design examples. IEEE Trans Ind Appl 48(6):2322–2332

2. Sarlioglu B, Morris CT, Han D, Li S (2017) Driving toward accessibility: a review of technological improvements for electric machines, power electronics, and batteries for electric and hybrid vehicles. IEEE Ind Appl Mag 23(1):14–25

3. Pellegrino G, Vagati A, Guglielmi P, Boazzo B (2012) Performance comparison between surface-mounted and interior PM motor drives for electric vehicle application. IEEE Trans Ind Electron 59(2):803–811

4. Yang Z, Shang F, Brown IP, Krishnamurthy M (2015) Comparative study of interior permanent magnet, induction, and switched reluctance motor drives for EV and HEV applications. IEEE Trans Transp Electr 1(3):245–254

5. Lipo TA, Du ZS (2015) Synchronous motor drives-a forgotten option. In: 2015 Intl Aegean conference on electrical machines and power electronics (ACEMP), 2015 Intl conference on optimization of electrical and electronic equipment (OPTIM) and 2015 Intl symposium on advanced electromechanical motion systems (ELECTROMOTION), Side, pp 1–5 (2015)

6. Dai J, Hagen S, Ludois DC, Brown IP (2017) Synchronous generator brushless field excitation and voltage regulation via capacitive coupling through journal bearings. IEEE Trans Ind Appl 53(4):3317–3326

7. Bilgin B et al (2019) Modeling and analysis of electric motors: state-of-the-art review. IEEE Trans Transp Electrif 5(3):602–617

8. Yao F, Sun D, Sun L, Lipo TA (2019) Dual third-harmonic-current excitation principle of a brushless synchronous machine based on double three-phase armature windings. In: Proceedings of 22nd international conference on electric machine systems (ICEMS), Harbin, China, pp 1–4

9. Ali Q, Lipo TA, Kwon B (2015) Design and analysis of a novel brushless wound rotor synchronous machine. IEEE Trans Magn 51(11):1–4

10. Ali Q, Atiq S, Lipo TA, Kwon B (2016) PM assisted, brushless wound rotor synchronous machine. J Magn 21(3):399–404

11. Hussain A, Kwon B (2018) A new brushless wound rotor synchronous machine using a special stator winding arrangement. Electr Eng 100(3):1797–1804

12. Hussain A, Atiq S, Kwon B (2018) Optimal design and experimental verification of wound rotor synchronous machine using subharmonic excitation for brushless operation. Energies 11(3):554

13. Rafin SMSH, Ali Q, Lipo TA (2022) A novel sub-harmonic synchronous machine using three-layer winding topology. World Electr Veh J 13(1):16. https://doi.org/10.3390/wevj13010016

14. S M Sajjad Hossain Rafin, TA Lipo, B Kwon (2014) A novel topology for a voltage source inverter with reduced transistor count and utilizing naturally commutated thyristors with simple commutation. In: 2014 international symposium on power electronics, electrical drives, automation and motion, Ischia, Italy, pp 643–648

15. Sajjad Hossain Rafin SM, Lipo TA, Kwon B (2015) Performance analysis of the three transistor voltage source inverter using different PWM techniques. In: 2015 9th international conference on power electronics and ECCE Asia (ICPE-ECCE Asia), Seoul, Korea (South), pp 1428–143